MINERALOGICAL MAGAZINE, SEPTEMBER 1978, VOL. 42, PP. 325-35

The growth of calcium metasilicate polymorphs from supercooled melts and glasses

R. M. WESTON AND P. S. ROGERS

Department of Metallurgy and Materials Science, Imperial College, London SW7 2BP

SUMMARY. The morphology of calcium metasilicate produced during the crystallization of glasses and melts of approximately metasilicate composition has been investigated. Both isothermal heat treatments and a dynamic crystal-pulling technique were employed. The crystallization took place by a dendritic or spherulitic mechanism, according to which of the crystal polymorphs is stable under the prevailing conditions. The morphology of the crystals is controlled by the ease with which the anionic groups present in the amorphous phase can be incorporated into the growing crystals. This is reflected in the values of the activation energies of crystal growth found for α-$CaSiO_3$ (160 kJ mol^{-1}) and for β-$CaSiO_3$ (319 to 383 kJ mol^{-1}). The Keith and Padden theory of spherulitic crystallization was verified for the growth of β-$CaSiO_3$ over a range of supercoolings. Time-temperature-transformation diagrams have been constructed from the experimental data.

IN the course of studies of the crystallization of glasses of approximately metasilicate composition it has been observed that spherulites containing fine fibres can be grown from internal nuclei (Mukherjee and Rogers, 1967), whereas when nucleation occurs only at a flat, external surface mutual impingement results in a more or less parallel alignment of the fibres (Williamson *et al.*, 1969). These observations led to the development of a dynamic crystallization technique (Maries and Rogers, 1975 and 1977), which can produce a unidirectionally crystallized rod containing a continuous array of parallel fibres. These materials have useful mechanical properties, and may be employed as reinforcement in certain types of composite. The mechanical and other physical properties are dependent upon the fibre morphology and may be optimized if this can be controlled. This paper describes a study of the factors controlling the crystallization characteristics of the fibrous phase.

There are three structural modifications of crystalline calcium metasilicate: wollastonite, parawollastonite, and pseudowollastonite. The low-temperature polymorph (β-$CaSiO_3$) may be wollastonite or parawollastonite. These are pyroxenoids (Prewitt and Peacor, 1964) in which chains of silicon-oxygen tetrahedra run parallel to the crystallographic *b* axis, the chain structure repeating after every three tetrahedra. The single chains are linked by calcium atoms in irregular octahedral coordination with six oxygen atoms. Monoclinic parawollastonite is related to the triclinic wollastonite by a simple packing modification (Tolliday, 1958), so that intergrowths of these two forms can occur on a sub-microscopic scale (Jeffery, 1953). The mineral is found as coarse, bladed aggregates, and is usually acicular or fibrous, even in small particles, the crystallographic *b* axis (chain axis) coinciding with the fibre axis (Andrews, 1970). The high-temperature polymorph pseudowollastonite (α-$CaSiO_3$) is generally regarded as being triclinic, but there are planes of pseudosymmetry perpendicular to all three triclinic unit-cell axes. The cell can therefore be regarded as pseudo-hexagonal, or a larger pseudo-orthorhombic cell (Jeffery and Heller, 1953). Some evidence exists for polytypism in α-$CaSiO_3$, which can be explained in terms of a double sandwich layer of $Si_3O_9^{6-}$ rings between hexagonally packed Ca^{2+} ions (Jeffery, 1964).

There is disagreement over the temperature of inversion of wollastonite to pseudowollastonite. Although this is usually taken as 1120 °C ± 10 °C, temperatures as high as 1190 °C and 1200 °C have been quoted (Andrews, 1970) (a small amount of diopside in solid solution is known to raise the inversion temperature). The rate of the inversion is said to be very slow below 1150 °C. Since the polymorphic forms of calcium metasilicate are relatively simple, and represent both ring and chain type structures, this was thought to be a suitable system for study.

Experimental

The crystallization of sixteen glasses of approximately metasilicate composition was investigated. Those compositions that produced the most exact alignment of surface-nucleated fibres in each system were selected. These compositions, expressed in terms of both weight and molecular percentages, are given in Table I. The glasses were prepared by using a standard technique that previous workers have found to give a homogeneous product (Williamson *et al.*, 1969). The final melt was either quenched and crushed or cast on to a metal plate, depending on whether the dynamic or isothermal heat treatment respectively was to be used.

TABLE I. *Glass compositions used to investigate the crystallization characteristics of calcium metasilicate*

Glass	Weight %					
	SiO_2	CaO	Al_2O_3	ZnO	Na_2O	CaF_2
I	50·9	29·6	12·0	7·4	—	—
II	55·0	35·0	5·0	—	5·0	—
IIF	54·7	29·9	4·3	—	4·3	6·8
III	50·0	30·0	—	20·0	—	—
	Mol %					
I	53·5	33·3	7·4	5·7	—	—
II	54·9	37·4	2·9	—	4·8	—
IIF	55·4	32·5	2·6	—	4·2	5·3
III	51·2	33·4	—	15·4	—	—

Isothermal heat-treatment technique. In order to provide suitable samples for the evaluation of isothermal crystallization behaviour, the cast glass blocks were cut into cubes of side approximately 1 cm. Glasses I, II, and IIF were crystallized isothermally. The cubes were contained in preheated firebrick trays fitted with chromel/alumel thermocouples and the heat treatments were timed from the moment when the thermocouple regained the equilibrium temperature after the tray had been loaded with samples. Initially the treatment was performed for a fixed time in the gradient region of a horizontal tube furnace to discover the optimum temperatures at which the more exact, isothermal measurements should be made. The glasses were then subjected to a series of isothermal tests in which several cubes were heated for various times at an accurately controlled temperature. The indentations in the firebrick trays were lined with alumina powder to prevent adhesion of the samples, which tended to soften and form beads when the heat-treatment temperature exceeded 900 °C. These tests were done in electric muffle furnaces in which the temperature could be controlled to within ± 3 °C using a thyristor regulator. Depending on the crystallization characteristics of a particular glass, the heat-treatment temperature was set at a value from 800 °C up to 1180 °C, and the specimens were heated for time intervals varying from 10 minutes up to 72 hours.

After heat treatment the cubes were sectioned normal to a flat face (the bottom surface in the cases where a bead had formed). One part was retained for Guinier powder X-ray analysis while the other was made into a thin section, suitable for examination by transmitted light microscopy.

Dynamic heat-treatment technique. Maries and Rogers (1975, 1977) have described a novel technique for directional devitrification from a molten zone (i.e. dynamic crystallization). A scaled-up version of this apparatus was constructed (Weston, 1977), see fig. 1. In this a slitted cylindrical platinum collar, 15 mm long and 5 mm in diameter, was connected between the water-cooled terminals of a 400 ampere output transformer. A recrystallized

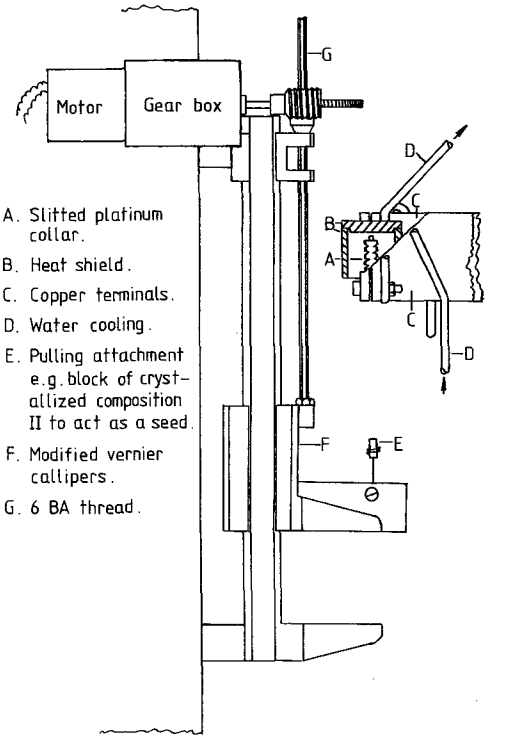

FIG. 1. Rod-pulling apparatus, dynamic heat-treatment technique.

alumina tube, of 25 mm internal diameter, was used as a heat shield around the collar, extending 5 mm above the top but only 1 mm below the bottom of the collar. An alumina lid could be fitted exactly into the top of the tube. The amount of power was controlled by a variable voltage transformer and this was sufficiently sensitive to set the collar temperature to within 10 °C. The collar was filled with the crushed glass and the power through the collar increased until the glass became fully molten and bubble-free. Surface tension forces held the melt inside the collar.

A motorized drive unit was constructed so that the melt could be pulled out of the bottom of the collar at a constant, known rate. The pulling connection, which also acted as the nucleation medium, could be a platinum wire spiral, a block (2 mm square cross-section) cut from a suitable isothermally crystallized metasilicate glass (glass II), which acted as a nucleation seed, a Pt/Pt 13% Rh thermocouple junction or a thermocouple junction together with a crystalline seed block.

A small, horizontal-slit air-blast outlet was fitted so as to be level with the bottom of the heat shield. The air blast increases the thermal gradient below the collar and allows rods of glass to be pulled from the melt in the collar at fast rates, without the glass necking off. However, differences in the thermal gradient also affect the devitrification characteristics of the rod.

The situation below the molten zone is represented in fig. 2. The rod cooling rate is a function of temperature to the fourth power (Maries and Rogers, 1978) and the corresponding growth-rate curve was found by Maries *et al.* (1975) using the glass composition III in Table I, which was that used for rod pulling. Once the crystals have nucleated and the pulling rate is constant, the growth front assumes a stable, steady-state position. Since this is crystal growth from the melt the crystal growth rate increases with decreasing temperature (i.e. increasing supercooling) and therefore if the growth rate exceeds the pulling rate of the rod, the crystal growth front approaches the molten zone and thus moves into a region at a higher temperature, the growth rate decreases, and the growth front drops back to the stable position. Conversely if the growth front drops down the rod the growth rate increases and the crystal growth interface moves up again to the stable position where the growth rate equals the pulling rate.

Calcium metasilicate, the primary devitrification product from the glass compositions used, has a phase transition that occurs in the same temperature range as that for crystallization. This means that relatively slow pulling rates will result in the crystallization of the high-temperature polymorph,

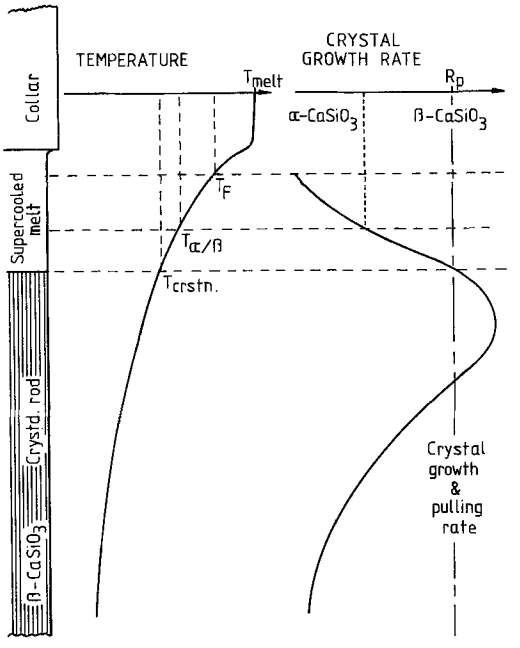

FIG. 2. Schematic diagram of dynamic crystal-pulling technique, showing rod cooling rate and crystal growth rate profiles operating below the molten zone.

and at greater speeds the low-temperature polymorph crystallizes until a speed is reached at which the rod quenches through the devitrification region and forms a glass.

Thin sections and specimens for powder X-ray analysis were prepared from sectioned 'rod' materials.

Results

Isothermal heat treatments. In the isothermally treated glasses I and II in Table I, crystallization was nucleated heterogeneously on an external surface with no evidence of the formation of internal nuclei, the crystals growing normal to the surface (orthotropically) into the glass. Both spherulitic- and dendritic-type crystallization were observed, modified by transcrystallization (mutual impingement on a flat surface) to give approximately parallel fibrous crystals, as shown diagrammatically in fig. 3.

From the systematic investigation of the isothermal unidirectional crystallization of calcium metasilicate in both the CaO–ZnO–Al_2O_3–SiO_2 and Na_2O–CaO–Al_2O_3–SiO_2 systems it was found that the compositions containing between 53 and 56 mol% silica gave materials with the most

perfectly aligned and undistorted fibrous microstructures. Too high a silica content resulted in materials containing broad, divergent fibres, for reasons discussed later. However, a sufficient silica content is necessary to give at least a small proportion of residual glass after heat treatment, in order to avoid thermal shock damage to the material on cooling from the fabrication temperature (Weston, 1977).

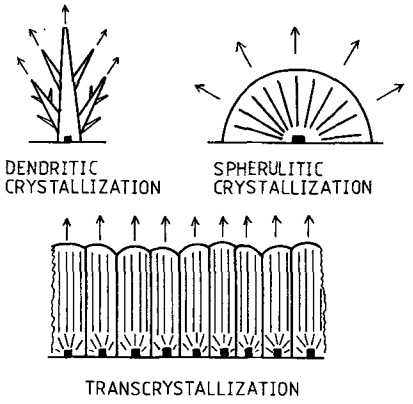

FIG. 3. Transcrystallization: mutual impingement between densely nucleated dendrites or spherulites on a flat surface restricts lateral crystal growth and gives a unidirectionally orientated fibrous microstructure.

A static, isothermal heat treatment was found to be suitable for the production of relatively large amounts of unidirectionally crystallized calcium metasilicate from glasses in which the maximum rate of crystal growth was 5 μm sec^{-1}. Of these, glasses I and II on devitrification gave the desired crystalline microstructures in the calcium aluminosilicate system in which the crystal growth rates were accelerated by the use of zinc oxide (Williamson, 1970; Williamson and Rogers, 1972) and sodium oxide additions respectively.

The crystal growth rate versus temperature curves for glass I are shown in fig. 4. On external surfaces that have been roughened by the action of the diamond wheel the high-temperature polymorph, α-$CaSiO_3$, tended to nucleate and grow in the form of primary dendrites even at temperatures substantially below the reported α/β transition temperature. Since β-$CaSiO_3$ is the equilibrium

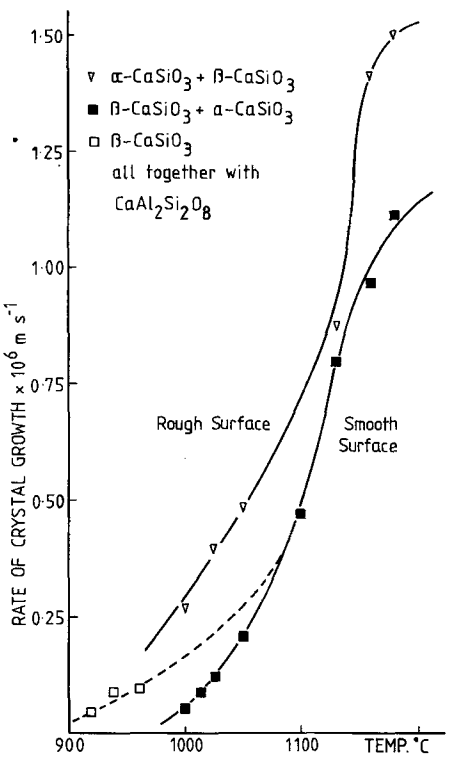

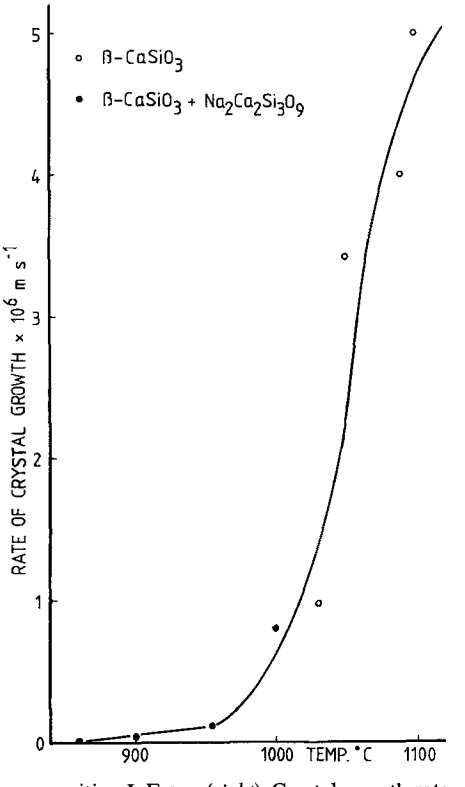

FIGS. 4 and 5: FIG. 4 (*left*). Crystal growth rate versus temperature, composition I. FIG. 5 (*right*). Crystal growth rate versus temperature, composition II.

phase below the transition temperature, then the driving force for nucleation (i.e. the difference in free energy between the molten state and the crystalline phase) of this polymorph will be greater than that for the nucleation of α-$CaSiO_3$. This may result in β-$CaSiO_3$ nucleating on a smoother surface than α-$CaSiO_3$, but since β-$CaSiO_3$ has a lower crystal growth rate than α-$CaSiO_3$ then on a rough surface on which both can nucleate, the faster-growing polymorph dominates the crystallization. In both cases $CaAl_2Si_2O_8$ was produced as a secondary crystallization product, nucleated at the interfaces between the sides of the primary fibres or dendrites and the residual glass.

The crystal growth rate versus temperature curve for glass II is shown in fig. 5. At all the isothermal heat-treatment temperatures investigated, β-$CaSiO_3$, nucleated at an external surface, was the primary crystallization product. The surface preparation of this glass did not affect the phase precipitated, possibly because the lower softening temperature of this glass makes all the sectioned surfaces smooth prior to nucleation. A sodium-calcium-silicate was given as a secondary crystallization product when samples were heat treated below 1000 °C.

Dynamic heat treatments. The dynamic, rod-pulling technique was employed with glasses that crystallized at greater than 10 μm sec^{-1} over the appropriate temperature range. However, Na_2O-CaO-SiO_2 glasses were found to be unsuitable for the production of β-$CaSiO_3$ by this method. The maximum crystal growth rate in these glasses occurs at a temperature above that of the α/β transition temperature and therefore as the pulling rate is increased only α-$CaSiO_3$ is precipitated until the maximum rate is exceeded when the rod quenches to a glass. In the CaO-ZnO-SiO_2 system, glass III had been found to have the maximum crystallization rate at a temperature below the transition temperature and had previously been established as suitable for the production of β-$CaSiO_3$ by rod-pulling (Maries *et al.*, 1975). By using this glass, and incorporating a thermocouple in the nucleation/pulling attachment, the variation of rod cooling rate and crystallization characteristics with pulling rate could be established, as shown in fig. 6. From these results a crystal growth rate versus temperature curve was constructed for β-$CaSiO_3$, fig. 7, and since the process was crystal

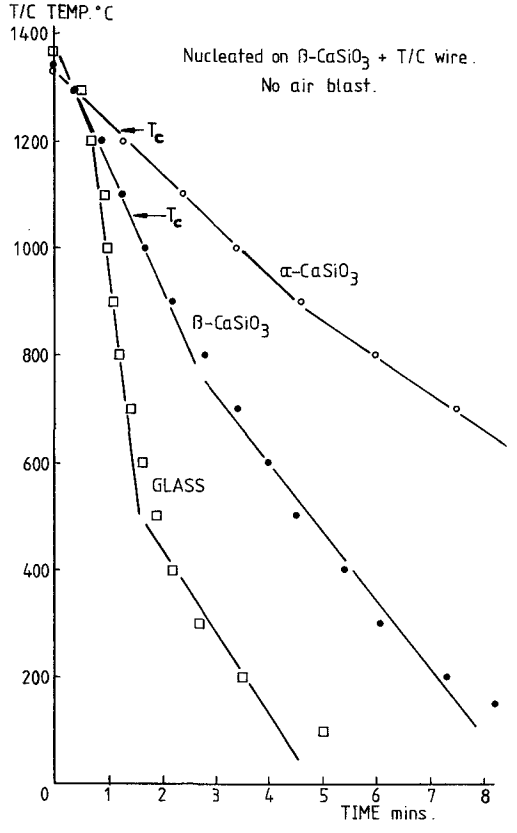

FIG. 6. Cooling rates of rods of composition III undergoing the dynamic crystallization technique. The nucleation agent was a β-$CaSiO_3$ block and a Pt/Pt 13% Rh thermocouple.

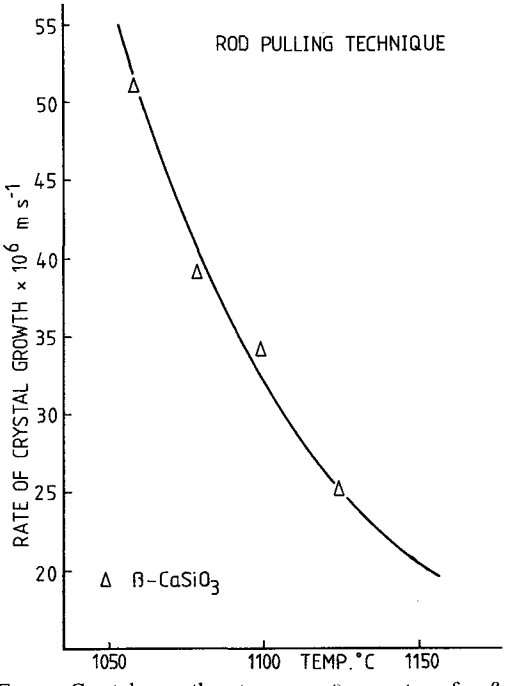

FIG. 7. Crystal growth rate versus temperature for β-$CaSiO_3$ rods pulled from composition III melts.

growth from a melt, this curve shows the growth rate increasing with decreasing temperature (i.e. above the temperature of maximum growth rate) unlike those in figs. 4 and 5. $Ca_2ZnSi_2O_7$ was given as a secondary crystallization product, particularly at low pulling speeds.

Time–temperature–transformation (t–T–T) diagrams were also constructed from the data, for nucleation both on a thermocouple junction only, and on a junction together with a β-$CaSiO_3$ seed crystal, figs. 8 and 9. From these it can be seen that the use of a seed crystal greatly increases the range of pulling speeds at which β-$CaSiO_3$ is given as the crystallization product, indicating that in this system the phase more easily nucleated continues to grow whether or not it is the 'stable' phase at the particular crystallization temperature.

Discussion

In every composition studied by either method it was found, with only one exception, that α-$CaSiO_3$ crystallized in the form of dendrites, either with or without secondary arms, and β-$CaSiO_3$ as fibres (i.e. fibres that would form spherulites but for transcrystallization), as shown in figs. 10 and 11. The spherulitic nature of the β-$CaSiO_3$ fibres was verified when glass IIF was heat treated to produce internally nucleated spherulites of β-$CaSiO_3$. The morphology and dimensions of the fibres making up the spherulites in composition IIF were closely matched by the aligned surface-nucleated fibres produced in glass II when isothermally heat treated at the same crystallization temperature, as can be seen by comparison of figs. 11 and 12. The only

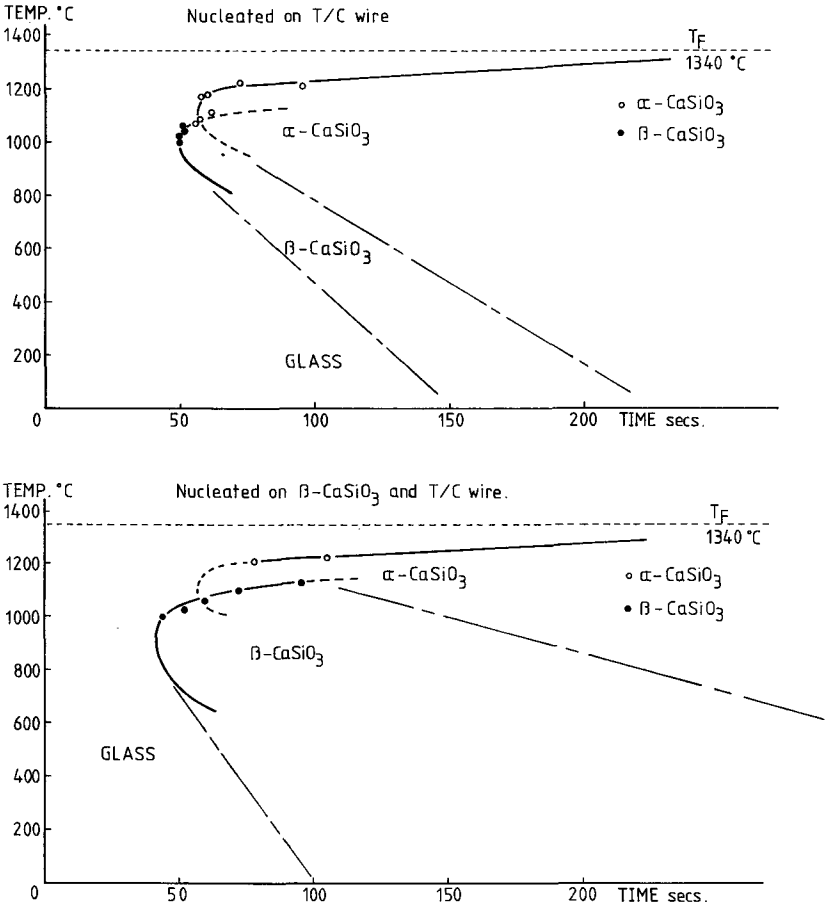

FIGS. 8 and 9: FIG. 8 (*top*). Time–temperature–transformation diagram for composition III rods nucleated on a Pt/Pt 13% Rh thermocouple. FIG. 9 (*bottom*). Time–temperature–transformation diagram for composition III rods nucleated on a β-$CaSiO_3$ block and a Pt/Pt 13% Rh thermocouple.

glass that produced α-$CaSiO_3$ in the form of this type of fibre was glass II when crystallized by the dynamic technique. Fig. 13 shows the quenched growth front of one of these rods, in which it is clearly seen that the fibre diameter decreased rapidly with temperature in agreement with the theory of spherulitic growth (Keith and Padden, 1963). The fibrous, as opposed to dendritic, morphology is thought to form in this case because of the shape of the crystal growth versus temperature curve for glass II just below the equilibrium crystallization temperature (T_F), see fig. 14. The glass II curve has a high rate of growth at temperatures just below T_F. (This is the type of curve found by Swift (1947) for the crystallization of calcium metasilicate from soda–lime–silica glass in which some silica had been replaced by alumina.) Therefore as the cold nucleation medium was placed in the melt in the collar, sufficient heat was extracted from this melt to cool the lower part below T_F and to form α-$CaSiO_3$ inside the collar prior to the rod being pulled. This polymorph continued to grow during rod-pulling, although the crystallization temperature fell as the rod was pulled below the heated collar. This resulted in α-$CaSiO_3$ crystallizing at an unusually low temperature and growing with the low-temperature fibrous morphology from the high viscosity melt.

Crystallization kinetics. Fig. 15 shows the coexistence of α-$CaSiO_3$ dendrites and β-$CaSiO_3$ fibres at a quenched crystal growth front in glass I. These two phases, nucleated as described above, grow in the same glass at the same temperature (in a medium of the same bulk viscosity), and therefore would have been supposed to have crystallized with the same morphology. However, it was found that α-$CaSiO_3$ crystallized more rapidly at a particular temperature. When the apparent activation energies of crystal growth (E_a) were calculated from Arrhenius plots, fig. 16 and Table II, that for the crystallization of α-$CaSiO_3$ was found to be only about half that required for β-$CaSiO_3$ growth. This difference may be explained by considering the amount of structural rearrangement necessary in

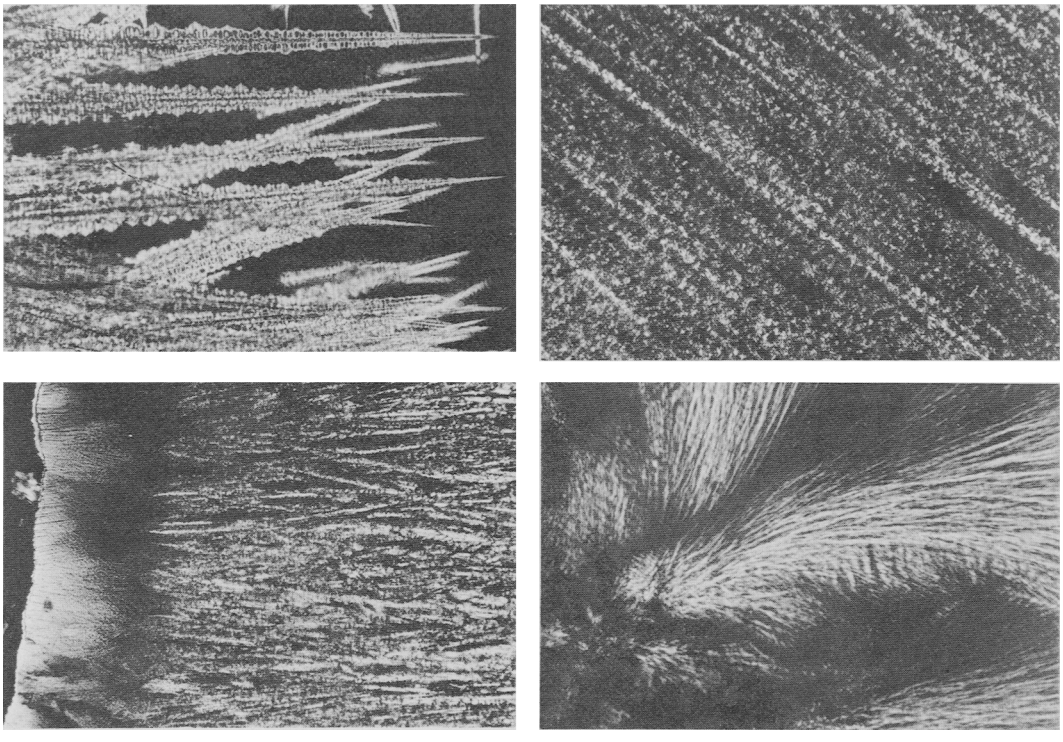

FIGS. 10–13: FIG. 10 (*top left*). Photomicrograph of α-$CaSiO_3$ dendrites grown at 1160 °C in glass I. × 150. FIG. 11 (*top right*). Photomicrograph of β-$CaSiO_3$ fibres grown at 1100 °C in glass II. × 500. FIG. 12 (*bottom left*). Photomicrograph of internally nucleated β-$CaSiO_3$ fibres forming spherulites, grown at 1100 °C in glass IIF. × 500. FIG. 13 (*bottom right*). Photomicrograph of composition II rod, pulled from 1470 °C at 20 $\mu m\ s^{-1}$, quenched growth front of α-$CaSiO_3$ fibres, showing semi-spherulites formed during quench. × 150.

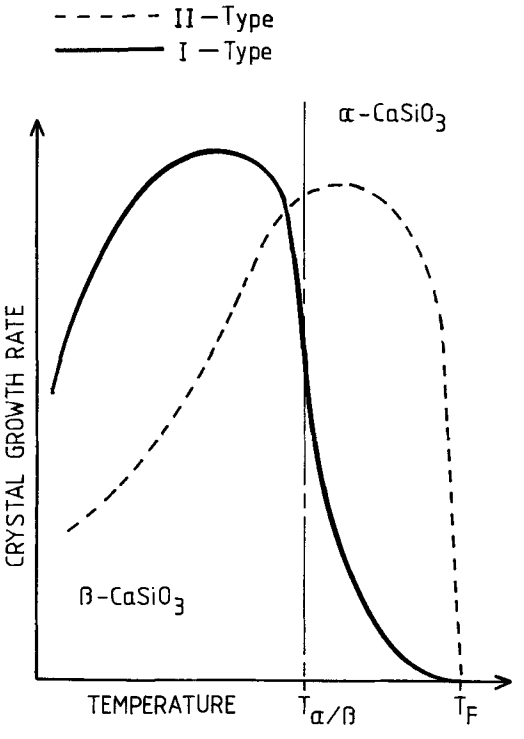

FIG. 14. Hypothetical crystal growth rate versus temperature curves.

the melt to orientate the molecular species such that they may join into the crystal lattice of the precipitating phase. A metasilicate melt contains $Si_3O_9^{6-}$ ring anions (Mackenzie, 1960) and these may be directly incorporated into the α-$CaSiO_3$ structure without the need to break strong bonds, i.e. only reorientation of existing structures is required for crystal growth to proceed. The β-$CaSiO_3$ structure, however, requires that the 'backbone' silica tetrahedra are arranged at the correct angles and are each linked to only two others and the silica network and ring structure in a metasilicate glass must be broken down before crystal growth can continue. This means that strong bonds must be broken and tetrahedra rotated in addition to simple reorientation, and therefore the effective viscosity of the glass is greater for the growth of β-$CaSiO_3$ as more energy is required to adapt the glass structure to the crystal structure. The crystallographic fibre orientation was found using long fibres produced by the rod-pulling technique for pinhole transmission X-ray analysis. The fibre axis corresponds to the [010] axis of the β-$CaSiO_3$ structure (the silica tetrahedra chain axis).

TABLE II. *Calculated apparent activation energies for crystal growth, E_a, and the derived activation energies for diffusion, E_D, for the crystallization of calcium metasilicate*

Composition	I	I	II	III
Crystallizing phase	α-$CaSiO_3$	β-$CaSiO_3$	β-$CaSiO_3$	β-$CaSiO_3$
Morphology	Dendrites	Fibres	Fibres	Fibres
E_a kJ mol^{-1}	160	319	383	—
E_D kJ mol^{-1}	—	368	456	319

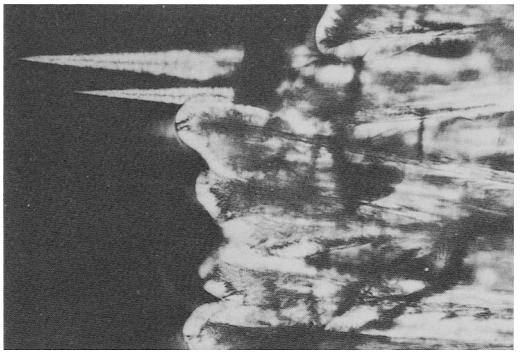

FIG. 15. Photomicrograph of β-$CaSiO_3$ fibres and α-$CaSiO_3$ dendrites (top) coexisting in composition I after isothermal heat treatment at 1160 °C. × 150.

The value of E_a for α-$CaSiO_3$ growth from glass I, 160 kJ mol^{-1} (see Table II), is in the same range as the activation energy for the diffusion of calcium ions through calcium aluminosilicate glass (Doremus, 1963), which suggests that diffusion of calcium across the boundary region at the interface is the major barrier to crystal growth. For β-$CaSiO_3$ growth from both glass I and glass II the E_a values are high, 319 kJ mol^{-1} and 383 kJ mol^{-1} respectively, and are in the same range of values as those obtained from studies of viscous flow in glasses near their crystallization temperatures (Williamson *et al.*, 1968), indicating that Si–O linkages are broken during crystal growth.

Variation of crystal morphology with undercooling. Lofgren (1974) found a change in crystal morphology with increasing supercooling in the crystallization of plagioclase crystals from the melt. At small degrees of supercooling (ΔT) tabular crystals formed. At progressively larger supercoolings skeletal crystals, then dendrites, appeared until finally spherulitic crystallization took place at high ΔT. These changes in morphology indicate that the

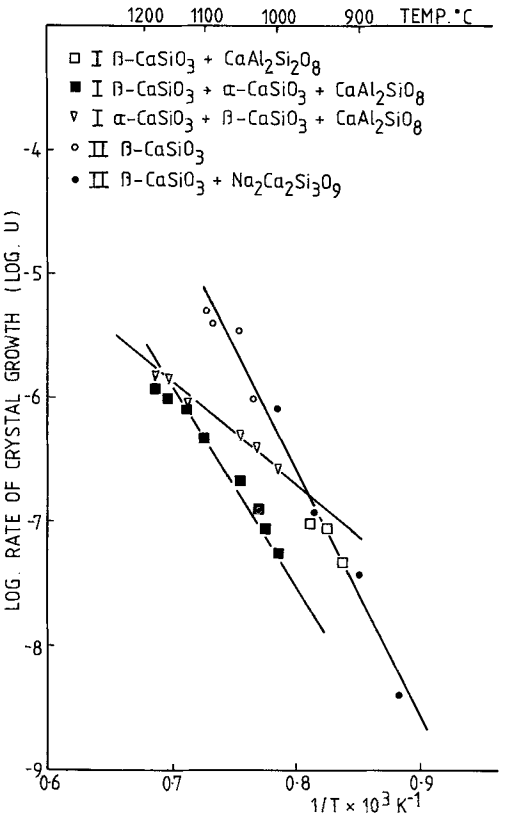

FIG. 16. Log crystal growth rate versus $1/T$ plots for compositions I and II.

stable width of a flat crystal/melt interface surface decreases with increasing supercooling. An unstable interface is formed when the crystal growth rate increases with distance into the melt and therefore any small perturbation on the growth front can quickly grow away from the rest of the crystal.

At typical supercoolings in viscous melts and particularly in glasses crystallized by reheating quenched samples, the crystal growth rate decreases with decreasing temperature, i.e. the crystallization temperature is below the maximum in the bell-shaped crystal growth rate versus temperature curves found in this type of material (Tammann, 1899). Most glass-forming melts do not precipitate crystals that have the same compositions as the glass and therefore material diffusion through the melt, both to and from the crystal/melt interface, is necessary for crystal growth. When a steady state is attained in this type of system there is an impurity-rich layer in the melt adjacent to the crystal growth front in which the equilibrium melting temperature is lowered with respect to that of the bulk of the melt. (The impurities are those substances included in different concentrations in the melt and the crystal and which therefore must be transported if the crystals are to grow.) Therefore the effective supercooling increases from the interface into the melt (see fig. 17) and this 'constitutional supercooling' (Rutter and Chalmers, 1953; Tashiro *et al.*, 1975) gives rise to an unstable interface, even in a substantially supercooled melt.

Bernauer (1929) suggested that impurities may be vital in order to produce spherulitic-type fibrous growth. Using Bernauer's work, Keith and Padden (1963) proposed a universal mechanism for spherulitic growth. They considered that when the steady state is established, in an unstirred melt, the impurity-rich layer formed has a thickness d, where $d = D/U$, D = diffusion coefficient of impurity in the melt, and U = crystal growth rate. This layer at the interface gives the constitutional supercooling described above. During spherulitic growth in viscous melts the crystal growth rate is relatively slow so that the temperature throughout the crystallizing system may be regarded as constant.

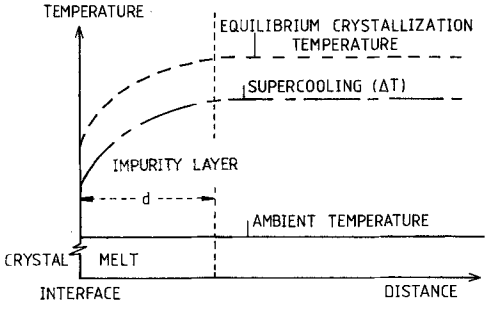

FIG. 17. Steady state situation at the crystal/melt interface in a supercooled melt in which additional constitutional supercooling has occurred.

Therefore as protrusions on the crystal/melt interface develop into fibres, the grooves of glass between them do not contain a steep temperature gradient at right angles to the fibre axis. This means that there will be an over-all decrease in supercooling throughout the grooves (the presence of impurities decreases the equilibrium crystallization temperature) and no significant temperature gradient, so that lateral growth into the grooves will be inhibited. The over-all result is that the morphology of the developing spherulites will be fibres separated by uncrystallized melt or glass. As the ambient temperature is lowered, or over long times at the higher temperature, secondary crystallization in the grooves may take place, but in some systems these grooves always remain as a glass. From consideration of the impurity diffusion

coefficients Keith and Padden calculated that the stable width of a fibre is approximately equal to the width of the impurity layer, *d*.

Dendritic crystal growth can arise from the steep temperature and concentration gradients around a developing protrusion when the crystal growth rate in the system is sufficiently rapid. In a glass-forming material this type of crystal morphology probably results as a combination of the effects of the evolution of latent heat and constitutional supercooling.

In the case of β-$CaSiO_3$ crystallization from a glass the rate-determining step is the diffusion of silicon through the melt. (The diffusion coefficients of Ca, Al, and Si through a calcium aluminosilicate slag have been found to be in the ratio of 1:4:10 respectively (Doremus, 1973).) Since the diffusion of silicon must involve the reorganization of the silica tetrahedra, this could be regarded as analogous to viscous flow. Diffusion is an activated process and can be represented by an Arrhenius equation: $D = B \exp(-E_D/RT)$ where B = a constant for a particular material, E_D = apparent activation energy for diffusion. Therefore E_D could be calculated from the slopes of log D versus $1/T$ plots, see fig. 18, D being found from the rate of spherulitic growth and the width of fibres produced at that growth rate. The values of E_D, see Table II, all fall in the activation energy range corresponding to viscous flow and for the diffusion of silicon through a silicate glass. The E_D results for glasses I and II are in relatively good agreement with the corresponding E_a values found for these glasses, indicating that both the crystal growth and diffusion energies are due to the necessity for the silica tetrahedra in the glass to be separated prior to incorporation of the tetrahedra in the growing crystal. This agreement could be taken as a verification of the Keith and Padden theory for spherulitic growth in silicate glass.

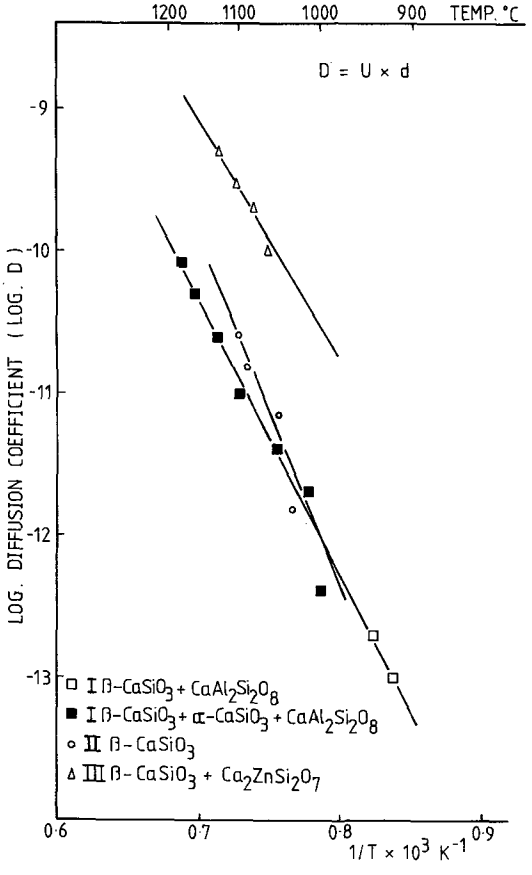

FIG. 18. Log D versus $1/T$ plots for spherulitic-type crystal growth in glasses I, II, and III.

The E_D value for glass III, crystallized by the dynamic technique, is lower than those found for the isothermally treated materials. In the rod-pulling method the melt ahead of the growth front is at a higher temperature than the crystallization temperature. It is therefore less viscous and can allow more rapid structural rearrangements at lower activation energies than is possible in the glass ahead of the crystals in isothermal growth.

Conclusions

A study of controlled crystallization in metasilicate glasses and melts has shown that the low temperature polymorph of calcium metasilicate gave materials with the most perfectly aligned fibres, since these fibres do not have any secondary arms and only branch at very small angles (non-crystallographic branching). This crystal morphology was usually only found in association with the low-temperature polymorph of calcium metasilicate, since spherulitic growth occurs in glasses and melts of high viscosity. Fibres between 5 and 50 μm in diameter were found to give the most perfect microstructures. Fibres that were too wide tended to be divergent since this morphology was associated with somewhat sparse surface nucleation, and also tended to have relatively low aspect ratios. Conversely, very fine fibres gave a structure consisting of an array of slightly divergent cones (segments of spherulites) and tended to recrystallize into lath-shaped crystals if the heat treatment was too prolonged, due to the extremely large surface area to volume ratio of narrow fibres.

Dendritic fibres only produced exact alignment in materials manufactured by the dynamic technique, when the development of secondary arms was somewhat inhibited. The primary dendrite

spines did not coarsen because the rods were pulled out of the crystal growth temperature region before this could occur. This crystal morphology was only found in association with the high-temperature polymorph of calcium metasilicate, since dendritic crystallization is given at intermediate values of supercooling.

Acknowledgements. The authors are grateful to the S.R.C. for the provision of a research studentship for one of us (R. M. W.). We wish to thank Dr. A. Maries for many useful discussions and Mr. A. J. Tipple for assistance with experimental techniques.

REFERENCES

Andrews (R. W.), 1970. *Wollastonite*, Institute of Geological Sciences, H.M.S.O., 1–6.

Bernauer (F.), 1929. *Gedrillte Kristalle*, Bornträger, Berlin.

Buckner (D.) and Roy (R.), 1955. *Geol. Soc. Am. Bull.* **66,** 1536–7.

Doremus (R. H.), 1963. *Modern Aspects of the Vitreous State*, **2,** London (Butterworths), 1–71.

—— 1973. *Glass science*, New York and London (Wiley Interscience), 170.

Jeffery (J. W.), 1953. *Acta Crystallogr.* **6,** 821–5.

—— 1964. *The Chemistry of Cements*, **1,** London (Academic Press), 138–42.

—— and Heller (L.), 1953. *Acta Crystallogr.* **6,** 807–8.

Keith (H. D.) and Padden (J. G.), 1963. *J. Appl. Phys.* **34,** 2409–21.

Lofgren (G.), 1974. *Am. J. Sci.* **273,** 243–73.

Mackenzie (J. D.), 1960. *Modern Aspects of the Vitreous State*, **1,** London (Butterworths), 188–218.

Mukherjee (S. P.) and Rogers (P. S.), 1967. *Phys. Chem. Glasses*, **8,** 81–7.

Maries (A.) and Rogers (P. S.), 1975. *Nature*, **252,** 401–2.

—— —— 1977. *Proc. 11th Internat. Congr. Glass*, Prague, **2,** 151–60.

—— —— 1978. *J. Mater. Sci.* (in press).

—— —— and Weston (R. M.), 1975. *Microstructure of Ceramics*, Abstracts of British Ceramic Society Convention, 18-1 to 18-3.

Prewitt (C. J.) and Peacor (D. R.), 1964. *Am. Mineral.* **49,** 1527–42.

Rogers (P. S.) and Williamson (J.), 1972. *Verres Réfract.* **26,** 53–6.

Rutter (J. W.) and Chalmers (B.), 1953. *Can. J. Phys.* **31,** 15.

Swift (H. R.), 1947. *J. Am. Ceram. Soc.* **30,** 170–4.

Tammann (G.), 1899. *Z. Phys. Chem.* **25,** 441.

Tashiro (M.), Kokubo (T.), Ito (S.), and Arioka (M.), 1975. *Bull. Inst. Chem. Res., Kyoto University*, **53,** 471–88.

Tolliday (J.), 1958. *Nature*, **182,** 1012–13.

Weston (R. M.), 1977. Ph.D. thesis, University of London.

Williamson (J.), 1970. *Mineral. Mag.* **37,** 759–70.

—— Tipple (A. J.), and Rogers (P. S.), 1968. *J. Iron Steel Inst.* **206,** 899–903.

—— —— —— 1969. *J. Mater. Sci.* **4,** 1069–74.

[*Manuscript received 21 October 1977, revised 23 February 1978*]